1. Łukasz Maciura[1], 2. Dariusz Wójcik[1], 3. Wojciech Rosa[2], 4. Tomasz Rymarczyk[1,3], 5. Michał Maj[1,3]

Netrix S.A., Research & Development Centre, Lublin, Poland (1), Lublin University of Technology, Lublin, Poland (2),
University of Economics and Innovation in Lublin, Poland (3)
ORCID: 1. 0000-0001-8657-3472; 2. 0000-0002-4200-3432; 3. 0000-0002-7051-6008; 4. 0000-0002-3524-9151; 5. 0000-0002-7604-8559

UNet model in image reconstruction for electrical impedance tomography

Streszczenie. Ten artykuł prezentuje nowy algorytm, gdzie sieć konwolucyjna UNet była użyta do korekcji wyników algorytmu deterministycznego jak było w podobnym rozwiązaniu używającym deterministyczny algorytm DBar. Zamiast algorytmu DBar inny algorytm rekonstrukcji EIT został użyty w kontekscie współpracy z tomografią impedancyjną w celu wyodrębnienia szczegółów rekonstrukcji EIT. Algorytm używa uczenie maszynowe do polepszenia obrazów tomograficznych uzyskanych za pomocą algorytmu deterministycznego. Artykuł pokazuje jak rekonstrukcja uzyskana za pomocą tomografu hybrydowego może być ulepszona by ukazywała więcej szczegółów. Celem tego artykułu jest zaprezentowanie rozwiązania, które będzie użyte w kontekscie tomografii medycznej, gdzie system EIT wraz z którym opracowany algorytm będzie użyty w celu uzyskania wysokiej rozdzielczości obrazów tomograficznych pęcherza moczowego.

Abstract. This paper presents a new algorithm where the UNet convolutional neural network was used to correct deterministic algorithm results, as was is another similar solution using the DBar deterministic algorithm. Instead of the DBar algorithm, another EIT reconstruction algorithm was used in the context cooperation with impedance tomography to extract details in EIT reconstruction. The algorithm uses machine learning to improve the tomographic images obtained with the deterministic algorithm. The final result contains much less noise, and the position of the objects is much better defined, unlike in the deterministic approach. Furthermore, the paper shows how the reconstruction obtained with the hybrid tomograph can be improved to show more details. This paper aims to present a solution that will be used in the context of medical tomography, where the EIT system and the developed algorithm will be used to obtain high-resolution tomography images of the bladder. (Model UNet w rekonstrukcji obrazu do elektrycznej tomografii impedancyjnej).

Keywords: *EIT* reconstruction, *UNet*, deep learning, convolutional neural networks.
Słowa kluczowe: rekonstrukcja *EIT*, *UNet*, uczenie głębokie, sieci konwolucyjne.

Introduction

The *EIT* reconstruction is a very hard (highly undetermined and ill-posed) problem to solve. It depends on the reconstruction of the image scene based on a vector obtained from multiple measurements using Electrical Impedance Tomography sensors. There are various *EIT* reconstruction algorithms in the literature. However, the best results could be obtained using neural networks (especially deep learning solutions).

Several AI methods could be used for such tasks. In the paper [1], the logistic regression using elastic net was used for *EIT* reconstruction. The paper [2] uses the ANN (artificial neural network) for image reconstruction. In the paper, the version of I neural networks trained for each output pixel separately was used for different pixels reconstruction. It generates better results than a single neural network, but the number of neural networks with all parameters per network is too big. Finally, in the paper [4], the sample of applied *CNN* network in *EIT* was shown.

The multiple nowadays *ANN EIT* reconstruction solutions are based on deep/convolutional autoencoders. One of these solutions is based on reconstruction obtained using another algorithm (D-Bar) and uses a deep convolutional autoencoder to correct these solutions [3]. The advantage of this method is that training input and output data are images and that we can use this method to correct results from other reconstruction methods.

The method based on deep autoencoders is described in the paper [7]. This paper uses deep autoencoders to reconstruct lungs object based on *EIT*. The method consists of three stages:
1) Training deep convolutional autoencoder using output images (in the research, lungs images were used)
2) The codes in the form of the vector obtained using the previous step are used as outputs for a training network containing a fully connected layer to generate such vectors based on vectors representing electric potentials from *EIT* sensors.

3) The final stage is a combination of two networks trained earlier. The output of the second network is put into the encoder part of the autoencoder trained in the first step. As a result, the network is created that can generate *EIT* reconstructions based on electrical potentials from *EIT* measurements.

There are many numerical methods [16-21]. Tomography makes it possible to analyse processes occurring in an object without interfering with them [22-25]. This paper was inspired by the *Deep DBar* method [3], which depends on deep learning correction of DBar *EIT* reconstruction algorithm [12] using *UNet 2D* convolutional model [13] with modification. Unfortunately, after testing the DBar algorithm, one can conclude that its speed is relatively very low, so a significantly faster solution should be developed for some practical applications.

After testing various models, we found a different useful DNN for EIT reconstruction based on autoencoder, described in detail in [10], [11]. This network consists of two parts (called *SAE* and *LR*) trained separately. *SAE* is the coder part of the trained earlier autoencoder to code the potential values, and LR is logistic regression layers.

The *SAE* (stacked) autoencoder training process contains several repeatable steps. All steps are trained to encode *EIT* potentials vector so have potentials vector at the input and output. First, the autoencoder contains only 3 layers (input, hidden and output layers). The hidden layer of this network contains the first stage encoded vector used in the next stage, input, and output. After several repetitions of that process, we trained a deep autoencoder with multiple hidden layers to encode vectors with potentials. Finally, the encoder part of the SAE autoencoder is used in the final model together with the LE layers.

Impedance hybrid tomograph

The hybrid tomograph combines two electrical tomography techniques: capacitive (*ECT*) and impedance (*EIT*). It can perform measurement cycles alternately or examine objects using only one of the methods. It makes it

suitable for both dynamic (*ECT*) and slower states more accurately (*ECT + EIT*). The device has its memory, on which it records the measurement results. It can also send them in real-time via the *Ethernet* or *USB* port, enabling interfacing with *Big Data* systems and/or databases. Details of data transmission are described on the following pages of this document.
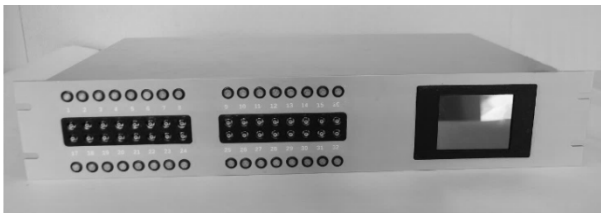

Fig. 1. The prototype of hybrid tomograph that has the functions of the final production device

The prototype of the device is shown in Figure 1. The device's size is only dictated by the chassis we used, and the final device will be no larger than a 5 cm cube.

Training data generation

The training datasets used in these experiments are synthetic data. The data generation algorithm generates 150 thousand scenes with artificial inclusions (circle, square or both - each subset containing 50 thousand samples) and noise. The conductivity of circles is smaller, and the conductivity of squares are bigger than background conductivity. These conditions are similar to conditions in the laboratory where real data were obtained. For each scene image, the *EIT* simulation was run, and potential vectors with 192 were generated.

The generation of synthetic training data for *EIT* reconstruction is a challenging problem (reverse to reverse problem) because this data should be very similar to real data obtained from the *EIT* laboratory. To obtain potential vectors based on generated scenes with circles and squares, the *EIT* simulation algorithm by means finite element method with square shapes was used. The parameters of the simulation algorithm for training dataset generation used in the experiments were tuned to obtain synthetic data like real data we have obtained as well as possible. The obtained potential vectors are used to calculate differential potentials vectors:

$$(1) \qquad X_i = x_i - x0i$$

where:x - is obtained potential vector for the scene with inclusions, x0i - is obtained potential vector for the scene without any inclusion, X - is the differential potential vector, i - is the index of potential vectors and differential potential vectors elements.

The generated 150 thousand samples of reference scene images (further called *Y*) and differential potential vectors (further called *X*) were divided into a training dataset (containing 120 thousand samples) and a test dataset (containing 30 thousand samples).

Initial EIT reconstructions using deterministic algorithm

For differential potential vectors in each sample in training and test datasets, the initial EIT reconstructions using the deterministic algorithm described below were generated in *80x80* images. The initial reconstructions (based on differential potential vectors as inputs) were performed using Kotre's regularization [14] using sensitivity matrix pseudo-inversion:

$$(2) \qquad J^{-1} = \left(J^T J + \lambda R \right)^{-1} J^T, R = \left(I \cdot \left(J^T j \right) \right)^{\frac{1}{2}}$$

where: *J* - is the sensitivity matrix; λ - is the regularization factor designated using gradient method, (·) - is an element wise multiplication operator.

Reconstructed conductivity is designated by:

$$(3) \qquad \sigma = J^{-1} V$$

where *V* – is differential measurement.

Preprocessing of data

The data during the research is normalized in the following way. The differential potential vectors used to generate initial *EIT* reconstructions using the algorithm described in the previous section are not normalized. Instead, the reference images were normalized to be in range <0,1> where background pixels values equal 0.5 while objects with conductivity smaller than background have pixels values equal 0.0 (circles) and objects with conductivity bigger than background (squares) have pixels values equal 1.0. The reference images are also processed to remove the external background generated by *EIT* simulation software (the proper pixels are inside the circle area surrounding electrodes).
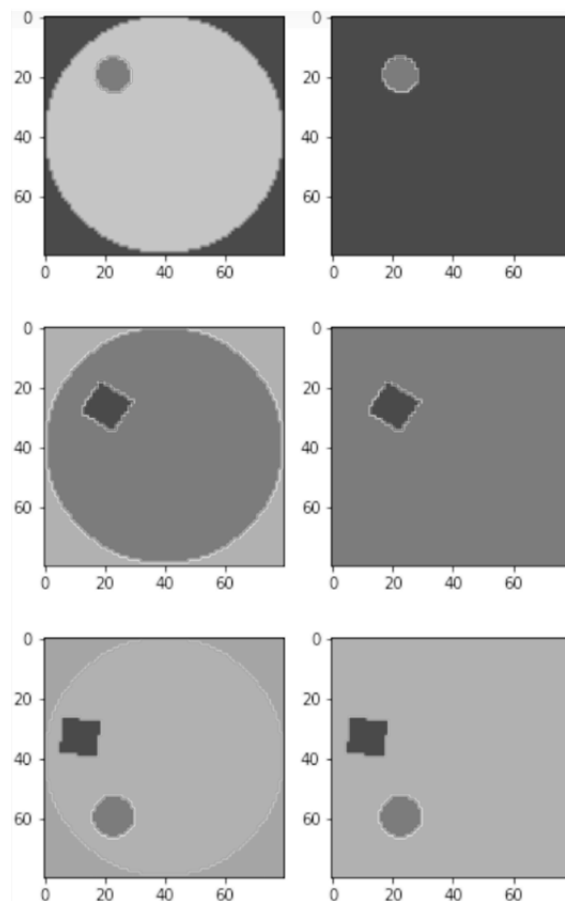

Fig. 2. The samples of reference images before and after external background removal

Because convolutional neural networks take the whole image area into account, the images should have a homogeneous background. In Figure 2, there are samples of reference images before the external background removal process and after that

The *EIT* reconstruction images (obtained in the way described in the previous section) are normalized using min-max for each image-sample in all datasets separately. This way of normalization is chosen based on previously

performed experiments with training autoencoder to encode *EIT* reconstruction images, and during the analysis of data the difference between maximal and minimal values in separate images was too big. So, the min-max normalization is performed per each pixel in the preprocessed image:

$$(4) \qquad p_{norm} = \frac{p - p_{min}}{p_{max} - p_{min}}$$

where: p - is the given pixel from the EIT reconstruction image after preprocessing, p_{min} - is the minimal value of all pixels in the image, p_{max} - is the maximal value of all pixels in the image, p_{norm} - is the given pixel value after normalization.
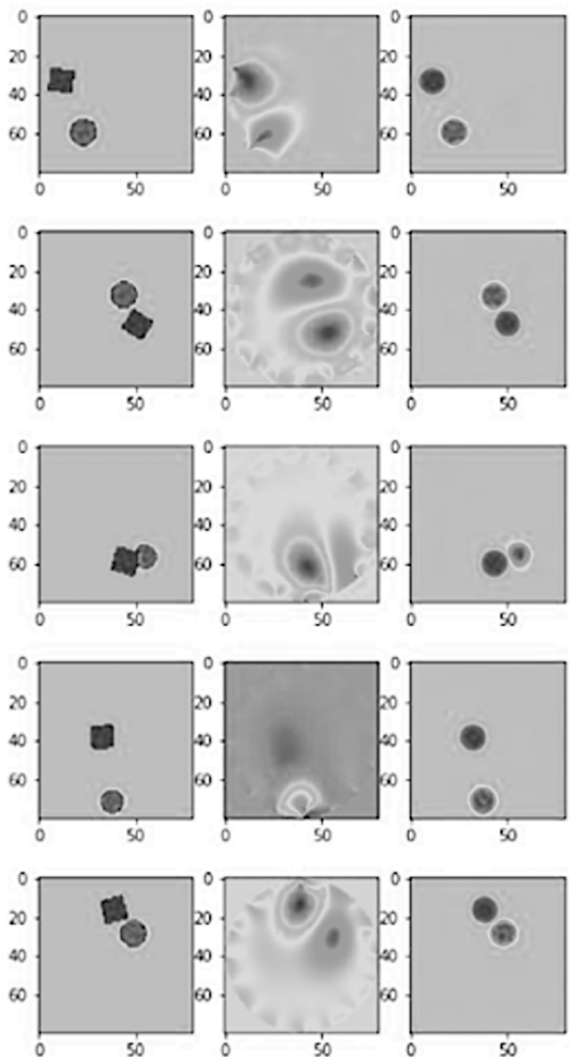

Fig. 3. Sample network results (columns: 1 – reference images, 2 – initial EIT reconstructions, 3 – network outputs)

Correction of EIT reconstructions using deep learning

This section describes experiments that led to *EIT* reconstruction corrections using a model similar to *UNet* [13].

Fig. 4. Results of the first and second steps of the post-processing algorithm of UNet model responses for each real data dataset.

Because of unable to train the standard *UNet* model with convolutions sizes to equal 3x3, these convolution filter sizes were changed to values 5x5 similar as was in the paper [3]. In the last layer of the network, the soft sign activation function was used.

The training process was performed on 120 thousand pairs of images (initial *EIT* reconstructions generated using deterministic algorithm at the input and reference images at the output). Both input and output images have sizes 80x80. In the training process, we are using *ADAM* optimizer with a learning rate equal 10^{-4}, mean squared error loss function, batch size equal 64 and 5 training epochs. After training on the training data set, we are obtaining on the test data set *MAE* metric equal 0.0079 and *DICE* [15] metric (calculated for circles and squares separately) 88.28%.

The used, modified version of the DICE metric is defined by the equation:

$$(5) \qquad DSC = \frac{2(TP_c + TP_s)}{2(TP_c + TP_s) + (FP_c + FP_s) + (FN_c + FN_s)}$$

where TPc, TPs, FPc, FPs, FNc, and FNs are true positives, false positives, and false negatives (for circles and squares). These values are calculated by logical operations on the binary images after thresholding of predicted and reference images for circles and squares separately.

The sample results obtained on the test data set we can see in Figure 3. In the image, we can see 5 samples of EIT reconstruction correction (for simultaneously circles and squares). Each sample contains 3 images (from left to right): reference image, initial *EIT* reconstruction using a deterministic algorithm, *UNet* model output (*EIT* reconstruction correction). Figure 4 shows the samples for each data set after the first (mean) and second (threshold) post-processing steps using all the samples in a given real data set.

Summary

We showed how to construct an algorithm that uses machine learning to enhance the tomographic images obtained with the deterministic algorithm. The final result contains much less noise, and the position of the objects is much better defined, unlike in the deterministic approach. This study aimed to develop and present the technology that will be used in the medical application. The goal is to obtain a reconstruction of the bladder so that it will be possible to calculate its volume in real-time, using the described hardware and the algorithms.

Authors:
dr inż. Łukasz Maciura E-mail: lukasz.maciura@netrix.com.pl,
dr inż. Dariusz Wójcik E-mail: dariusz.wojcik@netrix.com.pl,
Netrix S.A., Research & Development Centre, Lublin, Poland
Mgr inż. Wojciech Rosa E-mail: wrosa@pollub.pl
dr hab. inż. Tomasz Rymarczyk, prof.
mgr inż. Michał Maj
Netrix S.A, Reseach & Development Centre, Lublin, Poland
University of Economics and Innovation in Lublin, Poland

REFERENCES
[1] Kozłowski E., Rymarczyk T., Kłosowski G., Cieplak T., Logistic regression in image reconstruction in electrical impedance tomography, *Przegląd Elektrotechniczny*, 96 (2020), No. 5, 95-98
[2] Kłosowski G., Rymarczyk T., Tchórzewski P., Bednarczuk P, Kowalski M., - Neural hybrid tomograph for monitoring industrial reactors, *Przegląd Elektrotechniczny*, 96 (2020), No. 12, 190-193
[3] Hamilton S. J. Hauptmann, A., Deep D-bar: Real time Electrical Impedance Tomography Imaging with Deep Neural Networks, *IEEE Trans. Med. Imaging,* 37 (2018), No. 10, 2367 - 2377
[4] Kłosowski G., Rymarczyk T., Kania K., Świć A., Cieplak T., Maintenance of industrial reactors supported by deep learning driven ultrasound tomography, *Eksploatacja i Niezawodnosc –*

Maintenance and Reliability, 22 (2020), No. 1, 138–147

[5] Malone E., Sato dos Santos G., Holder D., Arridge S., A Reconstruction-Classification Method for Multifrequency Electrical Impedance Tomography, *IEEE Transactions on Medical Imaging*, 34 (2015), No.7, 1486-1497

[6] Khan T. A., Ling S.H., Review on Electrical Impedance Tomography: Artificial Intelligence Methods and its Applications, *Algorithms*, 12 (2019), No. 5, 1-18

[7] Seo J. K. et. al., Learning-Based Method for Solving Ill-Posed Nonlinear Inverse Problems: A Simulation Study of Lung EIT, *SIAM Journal on Imaging Sciences*, 12 (2019), No. 3, 1275-1295

[8] Fan Y., Ying L., Solving electrical impedance tomography with deep learning, *Journal of Computational Physics*, 404 (2020), 109119

[9] Fernandez - Fuentes X., Mera D., Gomez A., Vidal-Franco I., Towards a Fast and Accurate EIT Inverse Problem Solver: A Machine Learning Approach, *Electronics*, 7 (2018), No. 12, 422

[10] Li X., Lu Y., Wang J., Dang X., Wang Q., Duan X., and Sun Y, An image reconstruction framework based on deep neural network for electrical impedance tomography, In Proceedings of the *IEEE International Conference on Image Processing*, Beijing, China, 17–20 September 2017

[11] Li X. et. al., A novel deep neural network method for electrical impedance tomography, *Transactions of the Institute of Measurement and Control*, 41 (2019), No. 14, 4035–4049

[12] Hamilton S. J., Mueller J. L., Santos T. R., Robust computation in 2D absolute EIT (a-EIT) using D-bar methods with the' exp' approximation, *Physiological Measurement*, 39 (2018), No. 6, 1-17

[13] Ronneberger O., Fischer P., Brox T., U-Net: Convolutional Networks for Biomedical Image Segmentation, *Medical Image Computing and Computer-Assisted Intervention – MICCAI 2015.* 234-241

[14] Adler A., Dai T., Lionheart W., Temporal Image Reconstruction in Electrical Impedance Tomography, *Physiological Measurement*, 28 (2007), No. 7, 1-11

[15] Aziz Taha A., Hanbury A., Metrics for evaluating 3D medical image segmentation: analysis, selection, and tool, BMC Medical Imaging, 15 (2015), No. 29, 1-28

[16] Kłosowski G., Rymarczyk T., Niderla K., Rzemieniak M., Dmowski A., Maj M., Comparison of Machine Learning Methods for Image Reconstruction Using the LSTM Classifier in Industrial Electrical Tomography, *Energies*, 14 (2021), No. 21, 7269

[17] Kłosowski G., Rymarczyk T., Cieplak T., Niderla K., Skowron Ł., Quality Assessment of the Neural Algorithms on the Example of EIT-UST Hybrid Tomography, *Sensors*, 20(2020) No.11, 3324

[18] Łukiański, M., Wajman, R., The diagnostic of two-phase separation process using digital image segmentation algorithms, *Informatyka, Automatyka, Pomiary W Gospodarce I Ochronie Środowiska*, 10 (2020), No. 3, 5-8.

[19] Duraj, A.; Korzeniewska, E.; Krawczyk, A. Classification algorithms to identify changes in resistance. *Przegląd Elektrotechniczny*, 91 (2015), No.12, 82–84.

[20] Krawczyk A.; Korzeniewska E., Magnetophosphenes–history and contemporary implications. Przegląd Elektrotechniczny , 94 (2018), No.1, 61–64

[21] Mosorov V. Rybak G. Sankowski D., Plug Regime Flow Velocity Measurement Problem Based on Correlability Notion and Twin Plane Electrical Capacitance Tomography: Use Case, *Sensors*, 21 (2021), No.6, 2189 DOI: 10.3390/s21062189

[22] Rymarczyk T., Characterization of the shape of unknown objects by inverse numerical methods, *Przegląd Elektrotechniczny*, 88 (2012), No.7B, 138-140

[10] Rymarczyk T, Using electrical impedance tomography to monitoring flood banks 16th International Symposium on Applied Electromagnetics and Mechanics (ISEM), *International journal of applied electromagnetics and mechanics*, 45 (2014), 489-494

[11] Filipowicz SF, Rymarczyk T., The Shape Reconstruction of Unknown Objects for Inverse Problems, *Przegląd Elektrotechniczny*, 88 (2012), No.3A, 55-57

[12] Koulountzios P., Rymarczyk T., Soleimani M., A quantitative ultrasonic travel-time tomography system for investigation of liquid compounds elaborations in industrial processes, *Sensors*, 19 (2019), No. 23, 5117